

[文章编号] 1671-587X(2024)03-0749-10

DOI:10.13481/j.1671-587X.20240319

基于经皮冠状动脉介入治疗术后支架内再狭窄的免疫相关基因及免疫细胞浸润的生物信息学分析

冯玉飞¹, 金珊^{2,3}, 王玉冰^{2,3}, 鲁印飞¹, 庞丽娟^{2,3,4}, 刘克坚¹

(1. 石河子大学第一附属医院心内一科, 新疆 石河子 832000; 2. 石河子大学医学院病理系, 新疆 石河子 832000; 3. 石河子大学第一附属医院病理科, 新疆 石河子 832000; 4. 广东省湛江市湛江中心人民医院病理科, 广东 湛江 524000)

[摘要] **目的:** 筛选支架内再狭窄 (ISR) 中差异表达的免疫相关基因 (DEIRGs), 分析 ISR 中免疫细胞浸润情况, 并阐明 ISR 发生发展的机制。**方法:** 由基因表达数据库 (GEO) 下载 GSE46560 数据集样本 mRNA 基因表达数据, 分为 ISR 组与非 ISR (non-ISR) 组。采用 R 软件 “Limma” 包筛选出差异表达基因 (DEGs) 并与免疫相关基因 (IRGs) 交集获得 ISR 中 DEIRGs。采用 R 软件进行 DEIRGs 的基因本体论 (GO) 和京都基因与基因组百科全书 (KEGG) 富集分析, 采用 STRING 数据库构建蛋白-蛋白互作 (PPI) 网络, 以 Cytoscape 软件可视化并计算核心基因 (Hub 基因)。绘制 Hub 基因的受试者工作特征 (ROC) 曲线, 计算 ROC 曲线下面积 (AUC), 并评价其诊断价值。采用 CIBERSORT 软件分析 ISR 中免疫细胞浸润情况, Pearson 相关分析法分析免疫细胞间及其与关键基因之间的相关性。**结果:** 共鉴定出 331 个 DEGs ($P < 0.05$, $|\log_2FC| > 1$), 其中 176 个基因表达上调, 155 个基因表达下调, 获得 38 个 DEIRGs。GO 功能富集分析, 在生物过程 (BP) 中 DEIRGs 主要富集在防御反应、免疫反应和免疫系统; 在细胞组分 (CC) 中 DEIRGs 主要定位于胞外区和细胞质膜等; 在分子功能 (MF) 中主要参与调控信号受体结合和细胞因子受体活性等。KEGG 信号通路富集分析, ISR 中 DEIRGs 主要富集于磷脂酰肌醇 3-激酶/蛋白激酶 B (PI3K-AKT) 和转化生长因子 β (TGF- β) 等信号通路。PPI 网络, 前 10 位 Hub 基因中 CD19 具有最高节点。与 non-ISR 组比较, ISR 组样本中 CD19 mRNA 表达水平明显升高 ($P < 0.05$)。CD19 mRNA 表达的 ROC 曲线中 AUC 值为 0.92 ($P < 0.05$)。免疫细胞浸润分析, 与 non-ISR 组比较, ISR 组患者滤泡辅助性 T 淋巴细胞 (Tfh) 浸润水平升高 ($P < 0.05$), 初始 B 淋巴细胞、CD8+T 淋巴细胞、幼稚 CD4+T 淋巴细胞和 M0 巨噬细胞等浸润水平升高, 但差异无统计学意义 ($P > 0.05$), 记忆性 B 淋巴细胞、活化性记忆 CD4+T 淋巴细胞、调节性 T 淋巴细胞、静息性自然杀伤 (NK) 细胞、活化性 NK 细胞、单核细胞、静息性肥大细胞和中性粒细胞等浸润水平降低, 但差异无统计学意义 ($P > 0.05$)。Tfh 与 M0 巨噬细胞和静息肥大细胞等呈正相关关系 ($r = 0.88$, $P < 0.05$; $r = 0.68$, $P < 0.05$), 与单核细胞和中性粒细胞呈负相关关系 ($r = -0.49$, $P < 0.05$; $r = -0.42$, $P < 0.05$)。**结论:** CD19 可能通过调控 PI3K-AKT 信号通路激活影响 Tfh 和 B 淋巴细胞, 促进 ISR 的发生发展。CD19 可作为诊断 ISR 的生物标志物。

[收稿日期] 2023-06-09

[基金项目] 国家自然科学基金项目 (82060054); 新疆生产建设兵团科技局财政科技计划项目 (2020BC003); 广东省湛江市科技局科技发展基础研究专项 (2022A01028); 广东省湛江市科技局疾病防治重点项目 (2022A01103); 2022 年度湛江中心人民医院院级高层次人才科研启动经费项目 (2022A15, 2022A16); 石河子大学科研项目 (ZZZC202022A); 新疆维吾尔自治区研究生教育创新计划项目 (XJ2022G110); 石河子大学第一附属医院博士基金项目 (BS202205)

[作者简介] 冯玉飞 (1993—), 男, 河南省洛阳市人, 在读硕士研究生, 主要从事经皮冠状动脉介入治疗术后支架内再狭窄方面的研究。

[通信作者] 刘克坚, 教授, 主任医师, 硕士研究生导师 (E-mail: 25931884@qq.com); 庞丽娟, 教授, 主任医师, 博士研究生导师 (E-mail: ocean123456@163.com)

[关键词] 支架内再狭窄; CD19; 差异表达免疫相关基因; 免疫浸润; 生物标志物
[中图分类号] R392.12 [文献标志码] A

Bioinformatics analysis based on immune-related genes and immune cell infiltration of in-stent restenosis after percutaneous coronary intervention

FENG Yufei¹, JIN Shan^{2,3}, WANG Yubing^{2,3}, LU Yinfei¹, PANG Lijuan^{2,3,4}, LIU Kejian¹

(1. Department of Cardiology, First Affiliated Hospital, Shihezi University, Shihezi 832002, China;

2. Department of Pathology, School of Medical Sciences, Shihezi University, Shihezi 832000, China;

3. Department of Pathology, First Affiliated Hospital, Shihezi University, Shihezi 832000, China;

4. Department of Pathology, Zhanjiang Central People's Hospital, Zhanjiang City, Guangdong Province, Zhanjiang 524000, China)

ABSTRACT Objective: To screen the differentially expressed immune-related genes (DEIRGs) in in-stent restenosis (ISR), and to analyze the immune cell infiltration in ISR, and to clarify the mechanism of occurrence and development of ISR. **Methods:** The mRNA gene expression data of GSE46560 dataset samples were downloaded from the Gene Expression Omnibus (GEO), and divided into ISR group and non-ISR group. The “Limma” package in R software was used to identify the differentially expressed genes (DEGs) which were then intersected with immune-related genes (IRGs) to identify the DEIRGs in ISR; R software was used for Gene Ontology (GO) functional enrichment analysis and Kyoto Encyclopedia of Genes and Genomes (KEGG) signaling pathway enrichment analysis on DEIRGs; the STRING database was used to construct the protein-protein interaction (PPI) network, which was visualized and analyzed for Hub genes by Cytoscape software; the receiver operating characteristic (ROC) curve of the Hub genes were plotted, and the area under the curve (AUC) was calculated and the diagnostic value was evaluated; CIBERSORT software was used to analyze the immune cell infiltration in ISR; Pearson correlation analysis was used to analyze the relationships between the immune cells and the relationships between the immune cells and key genes. **Results:** A total of 331 DEGs were identified ($P < 0.05$, $|\log_2FC| > 1$), including 176 upregulated genes and 155 downregulated genes, and 38 DEIRGs were obtained. The GO functional enrichment analysis results showed that the DEIRGs were mainly enriched in biological processes (BP) such as defense response, immune response, and immune system; in cellular components (CC), the DEIRGs were located primarily in the extracellular region and cytoplasmic membrane; and in molecular functions (MF), the DEIRGs were mainly involved in regulating signaling receptor binding and cytokine receptor activity. The KEGG signaling pathway enrichment analysis results indicated that the DEIRGs in ISR were primarily enriched in the phosphatidylinositol 3-kinase/protein kinase B (PI3K-AKT) and transforming growth factor- β (TGF- β) signaling pathways. In the PPI network, CD19 had the highest node among the top 10 Hub genes. Compared with non-ISR group, the expression level of the CD19 gene in the samples in ISR group was increased ($P < 0.05$). The AUC value in the ROC curve of CD19 gene expression was 0.92 ($P < 0.05$). The immune cell infiltration analysis results showed that compared with non-ISR group, the infiltration level of T lymphocyte follicular helper (Tfh) cells in the patients in ISR group were increased ($P < 0.05$), the infiltration levels of immature B lymphocytes, CD8+T lymphocytes, naive CD4+T lymphocytes, and M0 macrophages were increased, but the differences were not statistically significant ($P > 0.05$), while the infiltration levels of memory B lymphocytes, activated memory CD4+T lymphocytes, regulatory T cells, resting natural killer (NK) cells, activated NK cells, monocytes,

resting mast cells, and neutrophils were decreased, but the differences were not statistically significant ($P > 0.05$). There were positive correlations between Tfh cells and M0 macrophages and resting mast cells ($r = 0.88, P < 0.05$; $r = 0.68, P < 0.05$), and there were negative correlations between Tfh cells and monocytes and neutrophils ($r = -0.49, P < 0.05$; $r = -0.42, P < 0.05$). **Conclusion:** CD19 may influence the occurrence and development of ISR by regulating the activation of the PI3K-AKT signaling pathway to affect the Tfh and B lymphocytes. CD19 can serve as a biomarker for the diagnosis of ISR.

KEYWORDS In-stent restenosis; CD19; Differentially expressed immune-related gene; Immune infiltration; Biomarker

目前全球范围内心血管疾病患病率处于持续上升阶段, 死亡率也居全球首位^[1]。经皮冠状动脉介入治疗术 (percutaneous coronary intervention, PCI) 是冠心病患者使用最广泛的血运重建方式, 但术后支架内再狭窄 (in-stent restenosis, ISR) 的发生率为 2%~10%^[2-4]。目前 ISR 发生的机制尚不明确。研究^[5-6]显示: 免疫炎症在 ISR 的发生发展中起重要作用, 可能是导致 PCI 术后 ISR 形成的重要因素。RNA 测序 (RNA sequencing, RNA-seq) 技术和生物信息学分析技术已成为研究基因交叉网络及识别诊断生物标志物的重要方法, 可用于探索 ISR 可能的发病机制和新的治疗靶点^[7]。本研究筛选 ISR 中差异表达的免疫相关基因 (differentially expressed immune-related genes, DEIRGs) 并分析

ISR 中免疫细胞的浸润情况, 采用生物信息学方法和 RNA-seq 技术探讨免疫炎症对 ISR 发生发展的影响, 为 ISR 的诊断和治疗提供参考。

1 资料与方法

1.1 数据来源 由基因表达综合 (Gene Expression Omnibus, GEO) 数据库 (<http://www.ncbi.nlm.nih.gov/geo>) 下载 ISR 微阵列数据集 GSE46560 的表达矩阵和平台信息^[8]。GSE46560 数据集来源平台为 GPL15207, 生物类型为人类, 时间为 2018 年, 包含 5 例 ISR 患者和 6 例非 ISR (non-ISR) 患者 mRNA 表达数据, 分别为 ISR 组和 non-ISR 组。GSE46560 数据集样本信息见表 1。

表 1 GSE46560 数据集样本信息

Tab. 1 Sample informations of GSE46560 dataset

Group	Sample	Source name	Sample type	Organism	Genotype	Age(year)
Non-ISR	GSM1132406	Blood	mRNA	Homo sapien	Male	55
	GSM1132407	Blood	mRNA	Homo sapien	Female	64
	GSM1132408	Blood	mRNA	Homo sapien	Male	75
	GSM1132409	Blood	mRNA	Homo sapien	Male	34
	GSM1132410	Blood	mRNA	Homo sapien	Male	78
	GSM1132411	Blood	mRNA	Homo sapien	Male	56
ISR	GSM1132412	Blood	mRNA	Homo sapien	Female	78
	GSM1132413	Blood	mRNA	Homo sapien	Male	58
	GSM1132414	Blood	mRNA	Homo sapien	Male	50
	GSM1132415	Blood	mRNA	Homo sapien	Male	56
	GSM1132416	Blood	mRNA	Homo sapien	Male	60

1.2 差异表达基因 (differentially expressed genes, DEGs) 筛选 对原始芯片数据进行归一化处理后, 采用 R 软件 “Limma” 包对 2 组样本基因进行差异表达分析。筛选标准为 $P < 0.05$ 和 $|\log_2FC| > 1$ 。采用 ggplot2 和 pheatmap 程序包对筛选出的 DEGs 进行可视化分析, 绘制热图和火山图。

1.3 免疫相关基因 (immune-related genes, IRGs) 和 DEIRGs 获取 由 ImmPort 数据库 (<https://immport.niaid.nih.gov>) 中获取 ISR 中 IRGs。将 DEGs 与 IRG 取交集, 获得 ISR 中的 DEIRGs, 并绘制韦恩图。

1.4 ISR中DEIRGs基因本体论(Gene Ontology, GO)功能和京都基因与基因组百科全书(Kyoto Encyclopedia of Genes and Genomes, KEGG)信号通路富集分析 按照参考文献[9]的方法,采用R软件ggplot2(v3.3.0)包、clusterProfiler(v3.14.3)包、org.Hs.eg.db(v3.10.0)包和enrichplot(v1.6.1)包对ISR中的DEIRGs进行GO功能及KEGG信号通路富集分析,并对分析结果进行可视化。

1.5 蛋白-蛋白互作(protein-protein interaction, PPI)网络构建及核心基因(Hub基因)筛选 将ISR中的DEIRGs输入STRING数据库(<https://string-db.org/>),构建PPI网络,以置信度 >0.9 作为PPI网络构建的标准。按照参考文献[10]的方法,采用Cytoscape软件(v3.9.1)对构建的PPI网络进行可视化,并利用CytoHubba插件计算Hub基因。

1.6 ISR中DEIRGs基因表达量验证和Hub基因诊断价值评价 获取GSE46560数据集中11个样本中关键基因表达量,采用GraphPad Prism绘制柱状图并进行可视化。采用GraphPad Prism绘制Hub基因的受试者工作特征(receiver operating characteristic curve, ROC)曲线,计算ROC曲线下面积(area under the curve, AUC),并评估其诊断价值。

1.7 免疫细胞浸润分析 CIBERSORT算法是一种多功能的反卷积算法,可进行免疫细胞浸润分析。采用R软件“CIBERSORT”包计算2组样本中22种免疫细胞浸润百分率。按照参考文献[8]中的方法进行可视化。采用Pearson相关分析法分析免疫细胞间及与关键基因之间的相关性。以 $P<0.05$ 为差异有统计学意义。

2 结果

2.1 2组样本DEGs鉴定 GSE46560数据集中共获得331个DEGs,其中176个基因表达上调,155个基因表达下调。见图1。

2.2 DEIRGs筛选 由ImmPort数据库获取1793个IRGs,将其与GSE46560数据集中获取的DEGs取交集后获得38个DEIRGs。前10位DEIRGs分别为白细胞介素1受体I(interleukin-1 receptor I, IL-1R1)、CC基序趋化因子受体3(C-C chemokine receptor type 3, CCR3)、CD19、分泌性白细胞蛋白酶抑制因子(secretory leukocyte

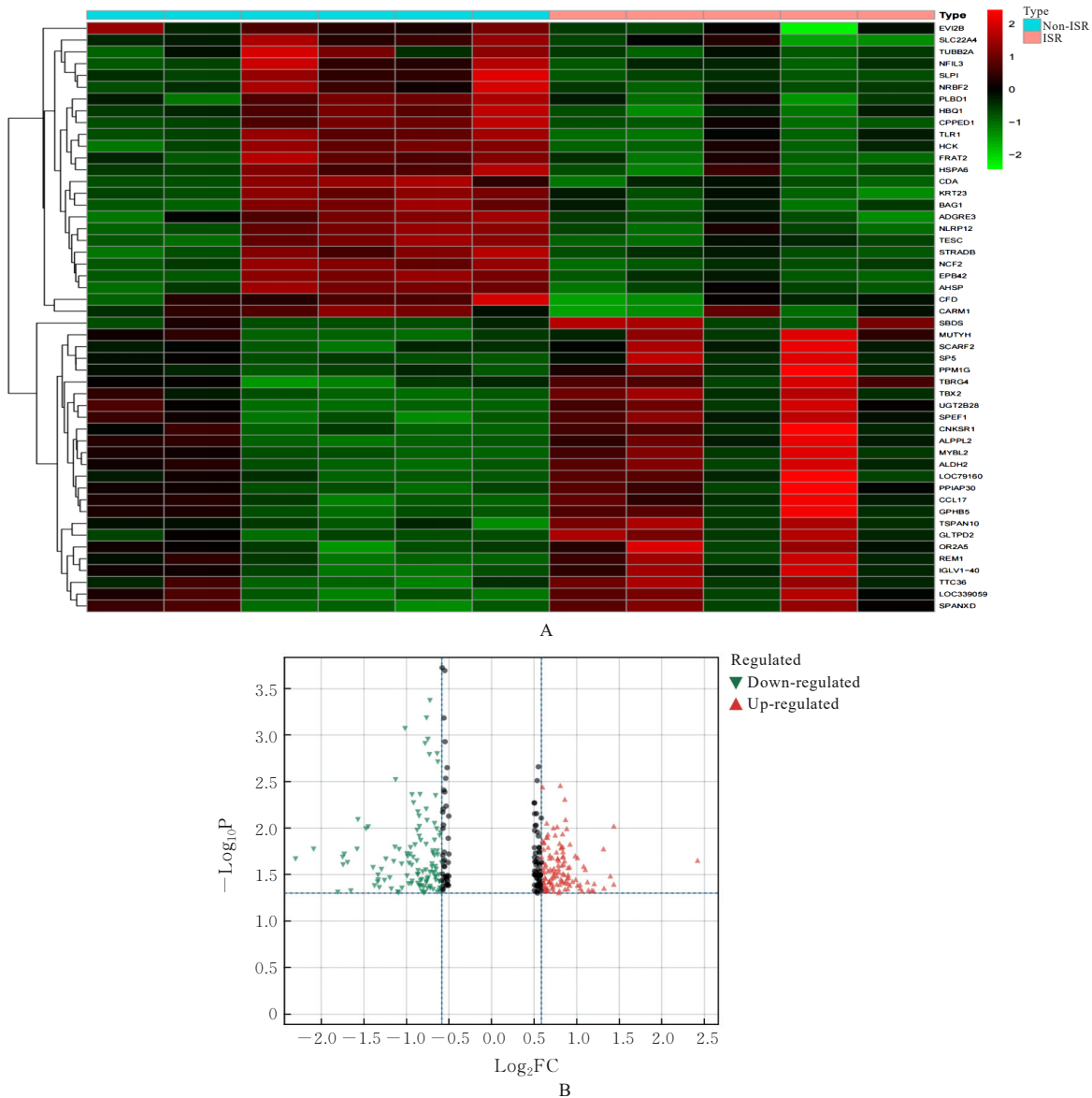
protease inhibitor, SLPI)、干扰素 $\alpha 6$ (interferon alpha-6, IFNA6)、肿瘤坏死因子受体超家族成员9(tumor necrosis factor receptor superfamily member 9, TNFRSF9)、酪氨酸激酶(spleen tyrosine kinase, SYK)、白细胞介素17受体A(interleukin-17 receptor A, IL-17RA)、白细胞介素10受体B(interleukin-10 receptor B, IL-10RB)和I型干扰素 α 受体1(interferon alpha receptor type 1, IFNAR1)。见图2和表2。

2.3 DEIRGs GO功能和KEGG信号通路富集分析 GO功能富集分析结果显示:生物过程(biological process, BP)中DEIRGs主要富集于防御反应、免疫反应和免疫系统;细胞组分(cellular component, CC)中DEIRGs主要定位于胞外区和细胞质膜;分子功能(molecular function, MF)中DEIRGs主要参与调控信号受体结合和细胞因子受体活性等。KEGG信号通路富集分析结果显示:DEIRGs主要富集于磷脂酰肌醇3-激酶/蛋白激酶B(phosphatidylinositol 3-kinase/protein kinase B, PI3K/AKT)信号通路、转化生长因子 β (transforming growth factor- β , TGF- β)信号通路和白细胞介素17(interleukin-17, IL-17)信号通路等。见图3。

2.4 PPI网络构建及Hub基因筛选 采用CytoHubba插件计算出前10位Hub基因,包括CD19、IL-1R1、SYK、IL-17RA和IFNAR1等均具有较高节点。见图4和表3。

2.5 Hub基因表达情况及诊断价值评价 与non-ISR组比较,ISR组样本中CD19 mRNA表达水平明显升高($P<0.05$),CD19 mRNA表达的ROC曲线中AUC值为0.92。见图5。

2.6 免疫细胞浸润和相关性分析 2组样本免疫细胞的组成以条形图显示。见图6A。与non-ISR组比较,ISR组患者滤泡辅助性T淋巴细胞(T lymphocyte follicular helper, Tfh)浸润水平升高($P<0.05$),初始B淋巴细胞、CD8 $+$ T淋巴细胞、幼稚CD4 $+$ T淋巴细胞和M0巨噬细胞等浸润水平升高,但差异无统计学意义($P>0.05$),记忆性B淋巴细胞、活化性记忆CD4 $+$ T淋巴细胞、调节性T淋巴细胞、静息性自然杀伤(natural killer, NK)细胞、活化性NK细胞、单核细胞、静息性肥大细胞和中性粒细胞等浸润水平降低,但差异无统计学意义($P>0.05$)。见图6B。Pearson相关分析结果



A: Heat map; B: Volcano map; Red: Up-regulated genes; Green: Down-regulated genes; Black: Genes with no significant differences.

图1 GSE46560数据集中ISR的DEGs

Fig. 1 DEGs of ISR in GSE46560 dataset

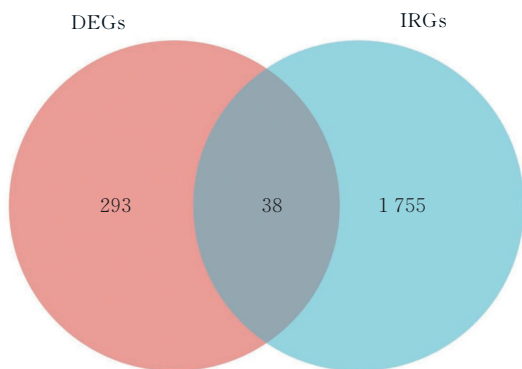


图2 GSE46560数据集中ISR的DEIRGs

Fig. 2 DEIRGs of ISR in GSE46560 dataset

显示: Tfh与M0巨噬细胞和静息肥大细胞呈正相关关系 ($r=0.88, P<0.05$; $r=0.68, P<0.05$), 与单核细胞和中性粒细胞呈负相关关系 ($r=-0.49, P<0.05$; $r=-0.42, P<0.05$)。见图6C。CD19与Tfh呈正相关关系 ($r=0.65, P<0.05$), 与 $\gamma\delta$ T细胞呈负相关关系 ($r=0.02, P=0.02$); SYK与嗜酸性粒细胞及M2巨噬细胞呈负相关关系 ($r=-0.03, P=0.03$); TNFRSF9与活化性记忆CD4+T淋巴细胞呈正相关关系 ($r=0.03, P=0.03$), 与M2巨噬细胞及嗜酸性粒细胞呈负相关关系 ($r=-0.03, P=0.03$; $r=-0.03, P=0.03$); CCR3与M2巨噬细胞2及

表2 GSE46560数据集中ISR的前10位DEIRGs
Tab. 2 Top 10 DEIRGs of ISR in GSE46560 dataset

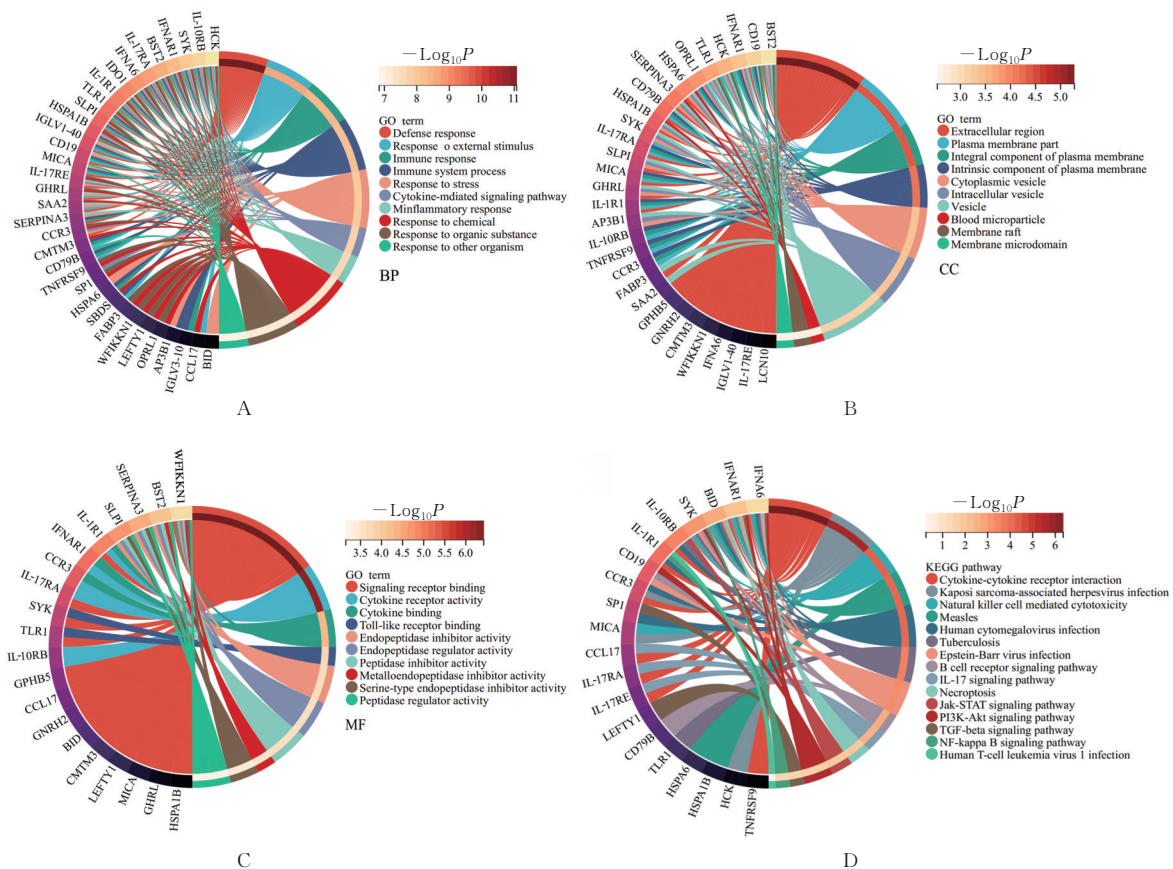
Rank	Gene	Log ₂ FC	P
1	IL-1R1	-0.729 984 494	0.001 589 458
2	CCR3	-0.848 170 488	0.009 625 487
3	CD19	0.821 019 788	0.015 127 227
4	SLPI	-1.580 539 076	0.016 843 607
5	IFNA6	0.609 176 376	0.023 118 319
6	TNFRSF9	-0.586 127 630	0.023 564 212
7	SYK	-0.692 433 588	0.029 734 058
8	IL-17RA	-0.549 992 248	0.032 917 596
9	IL-10RB	-0.572 143 770	0.042 174 389
10	IFNAR1	-0.782 222 264	0.048 843 759

嗜酸性粒细胞呈正相关关系 ($r=0.02$, $P=0.02$); IL-17RA与巨噬细胞及嗜酸性粒细胞呈负相关关系 ($r=-2.9e-4$, $P<0.01$); IFNA6与记忆性B淋巴细胞呈负相关关系 ($r=-6.4e-3$, $P<0.01$)。见图6D。

3 讨论

目前冠状动脉造影是诊断ISR病变及严重程度的金标准,但该方法为有创操作,面临一定风险^[12-13]。随着药物洗脱支架技术的引入和后续迭代,提高了PCI治疗的有效性和安全性,但ISR的发病率和由ISR产生的重复血运重建需求仍严重影响患者的预后^[9]。因此,需阐明ISR发生发展的机制并寻找有效的生物标志物,以降低PCI术后ISR的发生。研究^[14-17]显示:C反应蛋白和白细胞介素等免疫炎症因子、T淋巴细胞及B淋巴细胞等免疫细胞对ISR的发生发展起重要作用。此外,目前RNA-seq与生物信息学技术结合,已成为研究基因交叉网络和识别候选生物标志物的重要技术,可用于探索ISR可能的发病机制和新的治疗靶点。

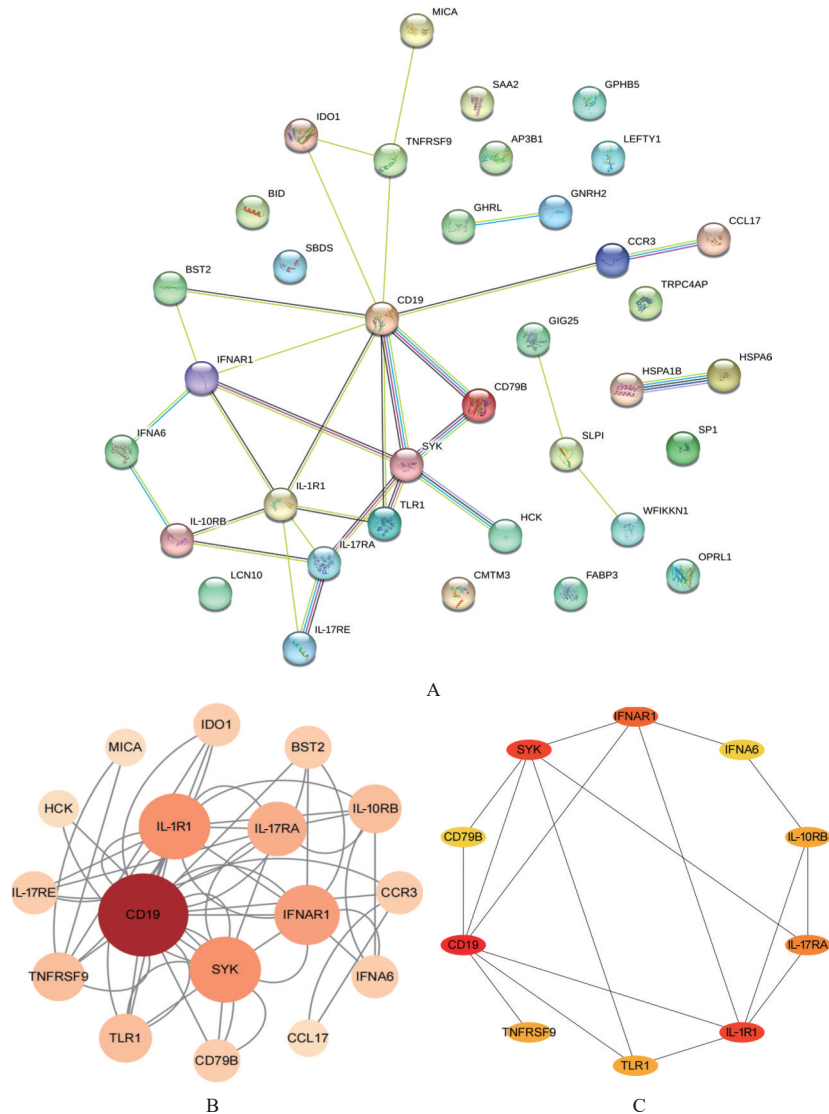
本研究通过GEO数据库,采用生物信息学技术分析ISR中的免疫炎症基因及免疫浸润特征,结果显示:筛选的DEIRGs与ISR的发生发展有密切关联。脂质链酶10 (lipocalin 10, Lcn10)^[18]、主



A—C: GO function enrichment analysis(A: BP; B: CC; C: MF); D: KEGG signaling pathway enrichment analysis.

图3 DEIRGs GO功能和KEGG信号通路富集分析

Fig. 3 GO functional and KEGG signaling pathway enrichment analysis on DEIRGs



A: PPI network of DEIRGs; B: Visualization analysis on DEIRGs; C: Top 10 Hub genes; Circle represented genes (The larger the circle, the higher the benign value of the darker colored nodes); Lines represented interactions between proteins encoded by genes.

图4 PPI网络图和DEIRGs可视化及前10位Hub基因

Fig. 4 PPI network map and DEIRGs visualization and top 10 Hub genes

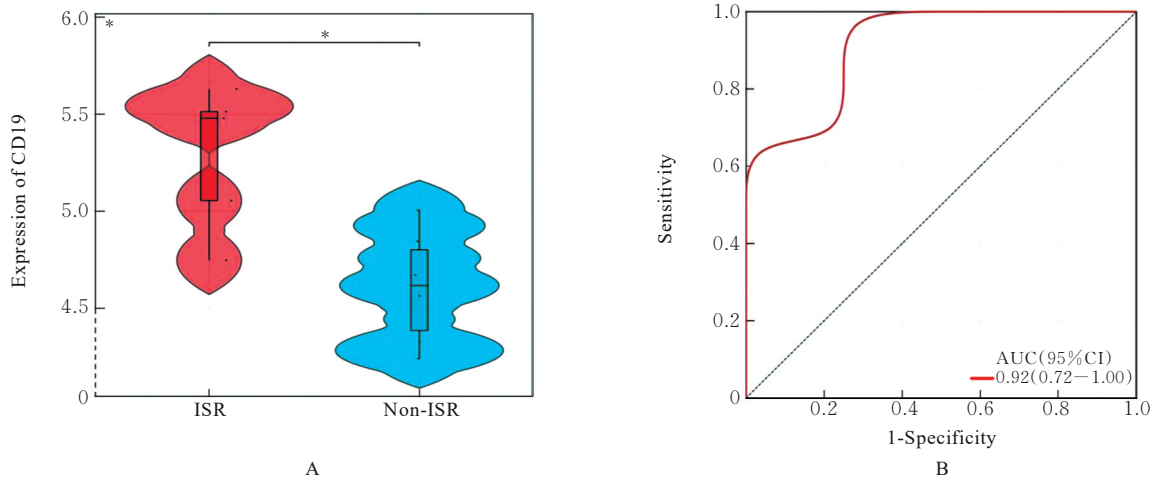
表3 CytoHubba插件筛选前10位Hub基因

Tab. 3 Top 10 Hub genes screened by CytoHubba plugin

Rank	Gene	Betweenness
1	CD19	140.833 330
2	IL-1R1	49.333 332
3	SYK	47.166 668
4	IFNAR1	30.500 000
5	TNFRSF9	30.000 000
6	CCR3	30.000 000
7	IL-17RA	12.666 667
8	IL-10RB	4.833 334
9	SLPI	2.000 000
10	IFNA6	1.666 667

要组织相容性复合体 I 类多肽相关序列 A (major histocompatibility complex class I polypeptide-related sequence A, MICA)^[19] 和白细胞介素 17 受体 E (interleukin-17 receptor E, IL-17RE)^[20] 等可通过调控免疫炎症参与 ISR 的发生发展。研究^[19]显示: MICA 与各种炎症和自身免疫性疾病有关, 可作为评估急性心肌梗死等心血管疾病严重程度的指标。Lcn10 可能在心血管疾病发病机制中发挥关键作用^[21-22]。

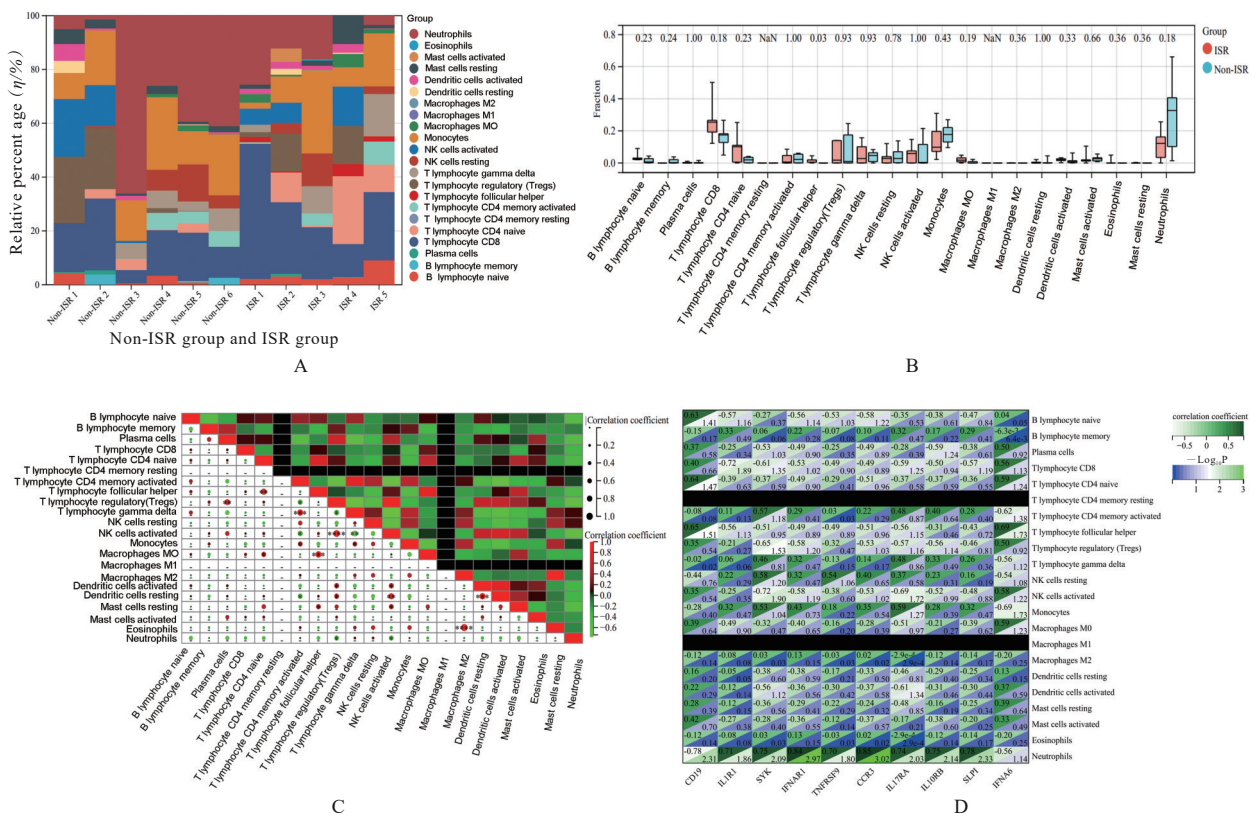
本研究结果显示: DEIRGs 主要定位于胞外区和细胞质膜, 可能通过参与 PI3K/AKT 和 TGF-β 等信号通路调控信号受体结合及细胞因子受体活性,



A: Differential expression of CD19 in samples in two groups; B: ROC curves. *P<0.05.

图5 CD19 mRNA 表达量验证及诊断价值评价

Fig. 5 Validation of CD19 mRNA expression amount and evaluation on diagnostic value



A: Relative percentage of 22 immune cells in each sample; B: Differences in immune infiltration between non-ISR and ISR samples; C: Relationship between immune cells; D: Correlation between hub genes and immune cells.

图6 免疫细胞浸润分析

Fig. 6 Immune cell infiltration analysis

参与防御反应和免疫反应等过程。PI3K/AKT 和 TGF-β等信号通路通过炎症等途径影响血管损伤后的新生内膜增生,进而影响 ISR 的发生发展^[14-17, 23]。研究^[24]发现:半夏可通过调控 PI3K/AKT 信号通

路,抑制炎症反应和增加内皮祖细胞(endothelial progenitor cells, EPCs)百分率,进而减少动脉粥样硬化大鼠颈动脉损伤后的新生内膜增生。PI3K/AKT 信号通路促进血管平滑肌细胞(vascular

smooth muscle cells, VSMCs) 的周期进展, 并在损伤诱导的新生内膜增生和ISR中起重要作用^[25]。TGF- β 1可能参与诱导内膜增厚, 在动脉血管损伤后, TGF- β 1上调导致各种下游途径激活, 进而刺激VSMCs的增殖和迁移及局部细胞外基质蛋白的产生, 导致ISR的发生。抑制TGF- β 1活性可减少动脉血管损伤后的内膜增厚, 从而减轻ISR^[26-27]。因此, DEIRGs可能通过PI3K/AKT和TGF- β 等信号通路调控免疫炎症及PCI术后的血管内新生内膜增生, 进而影响ISR的发生发展。

本研究结果显示: CD19具有最高节点, 可作为Hub基因。CD19作为在B淋巴细胞上表达的免疫球蛋白超家族的成员, 是B细胞抗原受体(B cell antigen receptor, BCR)信号转导的关键共受体, 可通过调控免疫炎症促进ISR的发生^[28-29]。研究^[30]显示: PI3K是CD19下游的效应分子, 二者结合促进了PI3K信号通路的激活。CD19与BCR结合后, B淋巴细胞中PI3K信号通路的数量是未结合B淋巴细胞中的10倍^[31]。绘制CD19的ROC曲线, 结果显示: AUC为0.92, 提示CD19可作为诊断ISR的生物标志物。KEGG信号通路富集分析结果显示: CD19富集于PI3K/AKT通路中, 提示CD19可能通过调控PI3K/AKT信号通路促进ISR的发生发展。

免疫细胞在ISR的发生发展中起重要作用, 免疫和炎症反应在血管机械损伤前期即被激活, 该过程通常伴随多种细胞因子和炎症介质的释放, 可诱导T淋巴细胞(包括T_H细胞和CD8⁺T淋巴细胞)、B淋巴细胞和巨噬细胞等向损伤部位趋化、黏附、聚集或极化, 进而共同导致新生内膜的增生, 最终形成ISR^[32-33]。本研究结果显示: 与non-ISR组比较, ISR组患者T_H的免疫细胞浸润水平升高。T_H细胞是为CD4⁺T淋巴细胞亚群的特殊类型的辅助性T淋巴细胞, 可促进B淋巴细胞成熟, 发挥免疫作用。研究^[34]显示: 在ISR小鼠模型中, T_H促进ISR的发生发展, 而T_H缺乏的小鼠ISR得到改善。PREITE等^[35]研究显示: PI3K的激活是T_H细胞发育所必需的条件, 选择性消除PI3K募集的p85结合位点突变可导致T_H细胞形成缺陷。

综上所述, Hub基因CD19可能通过调控PI3K/AKT信号通路的激活影响T_H和B淋巴细胞, 促进ISR的发生发展。CD19可作为诊断ISR的生物标志物。

利益冲突声明:

所有作者声明不存在利益冲突。

作者贡献声明:

冯玉飞参与研究设计、论文构思、数据分析和论文撰写, 金珊参与数据采集分析, 王玉冰和鲁印飞参与论文审阅, 庞丽娟和刘克坚参与研究项目指导。

[参考文献]

- [1] HOARE D, BUSSOO A, NEALE S, et al. The future of cardiovascular stents: bioresorbable and integrated biosensor technology[J]. *Adv Sci*, 2019, 6(20): 1900856.
- [2] ALFONSO F, GONZALO N, RIVERO F, et al. The year in cardiovascular medicine 2020: interventional cardiology[J]. *Eur Heart J*, 2021, 42(10): 985-1003.
- [3] ULLRICH H, OLSCHESKI M, MÜNZEL T, et al. Coronary In-stent restenosis: predictors and treatment[J]. *Dtsch Arztebl Int*, 2021, 118(38): 637-644.
- [4] YERASI C, CASE B C, FORRESTAL B J, et al. Drug-coated balloon for De Novo Coronary artery disease: JACC state-of-the-art review [J]. *J Am Coll Cardiol*, 2020, 75(9): 1061-1073.
- [5] NICCOLI G, MONTONE R A, SABATO V, et al. Role of allergic inflammatory cells in coronary artery disease[J]. *Circulation*, 2018, 138(16): 1736-1748.
- [6] BANAI S, FINKELSTEIN A, ALMAGOR Y, et al. Targeted anti-inflammatory systemic therapy for restenosis: The Biorest Liposomal Alendronate with Stenting Study (BLAST)—a double blind, randomized clinical trial[J]. *Am Heart J*, 2013, 165(2): 234-240.
- [7] YAO Y, YAN Z Y, LIAN S L, et al. Prognostic value of novel immune-related genomic biomarkers identified in head and neck squamous cell carcinoma[J]. *J Immunother Cancer*, 2020, 8(2): e000444.
- [8] 范吉林, 朱婷婷, 田晓玲, 等. 基于房颤中circRNA-miRNA-mRNA网络构建和免疫细胞浸润的生物信息学分析[J]. *吉林大学学报(医学版)*, 2022, 48(6): 1535-1545.
- [9] FAN J X, CAO S, CHEN M Y, et al. Investigating the AC079305/DUSP1 axis as oxidative stress-related signatures and immune infiltration characteristics in ischemic stroke [J]. *Oxid Med Cell Longev*, 2022, 2022: 8432352.
- [10] 张德洪, 郑明珠, 李家秋, 等. 基于MSR1 mRNA和蛋白在泛癌组织中表达的生物信息学分析及其意义[J]. *吉林大学学报(医学版)*, 2023, 49(2): 425-439.
- [11] 赵志娟, 孟 莲, 刘春霞. 基于融合基因作用于横纹肌

- 肉瘤的miRNA-mRNA调控网络的生物信息学分析[J]. 吉林大学学报(医学版), 2022, 48(1): 154-162.
- [12] GIUSTINO G, COLOMBO A, CAMAJ A, et al. Coronary In-stent restenosis: JACC state-of-the-art review[J]. J Am Coll Cardiol, 2022, 80(4): 348-372.
- [13] COLLET C, GRUNDEKEN M J, ASANO T, et al. State of the art: coronary angiography [J]. EuroIntervention, 2017, 13(6): 634-643.
- [14] DEMYANETS S, TENTZERIS I, JARAI R, et al. An increase of interleukin-33 serum levels after coronary stent implantation is associated with coronary in-stent restenosis[J]. Cytokine, 2014, 67(2): 65-70.
- [15] SCHILLINGER M, MINAR E. Restenosis after percutaneous angioplasty: the role of vascular inflammation[J]. Vasc Health Risk Manag, 2005, 1(1): 73-78.
- [16] DEL PORTO F, CIFANI N, PROIETTA M, et al. Lag3⁺ regulatory T lymphocytes in critical carotid artery stenosis[J]. Clin Exp Med, 2019, 19(4): 463-468.
- [17] DEL PORTO F, CIFANI N, PROIETTA M, et al. Regulatory T CD4⁺ CD25⁺ lymphocytes increase in symptomatic carotid artery stenosis [J]. Ann Med, 2017, 49(4): 283-290.
- [18] LI Q Q, LI Y T, HUANG W, et al. Loss of lipocalin 10 exacerbates diabetes-induced cardiomyopathy via disruption of Nr4a1-mediated anti-inflammatory response in macrophages[J]. Front Immunol, 2022, 13: 930397.
- [19] HAOHAN S, PUSSADHAMMA B, JUMNAINSONG A, et al. Association of major histocompatibility complex class I related chain A/B positive microparticles with acute myocardial infarction and disease severity[J]. Diagnostics, 2020, 10(10): 766.
- [20] GORCZYNSKI R M. IL-17 signaling in the tumor microenvironment[J]. Adv Exp Med Biol, 2020, 1240: 47-58.
- [21] DI SALVO T G, YANG K C, BRITTAI E, et al. Right ventricular myocardial biomarkers in human heart failure[J]. J Card Fail, 2015, 21(5): 398-411.
- [22] ALIMADADI A, MUNROE P B, JOE B, et al. Meta-analysis of dilated cardiomyopathy using cardiac RNA-seq transcriptomic datasets[J]. Genes, 2020, 11(1): 60.
- [23] ZHANG B, YAO R J, HU C, et al. Epigallocatechin gallate mediated sandwich-like coating for mimicking endothelium with sustained therapeutic nitric oxide generation and heparin release [J]. Biomaterials, 2021, 269: 120418.
- [24] LU H K, HUANG Y, LIANG X Y, et al. *Pinellia ternata* attenuates carotid artery intimal hyperplasia and increases endothelial progenitor cell activity via the PI3K/Akt signalling pathway in wire-injured rats [J]. Pharm Biol, 2020, 58(1): 1184-1191.
- [25] TANG Z H, WANG Y, FAN Y B, et al. Suppression of c-Cbl tyrosine phosphorylation inhibits neointimal formation in balloon-injured rat arteries [J]. Circulation, 2008, 118(7): 764-772.
- [26] KHAN R, AGROTIS A, BOBIK A. Understanding the role of transforming growth factor-beta1 in intimal thickening after vascular injury [J]. Cardiovasc Res, 2007, 74(2): 223-234.
- [27] WANG S X, LINCOLN T M, MURPHY-ULLRICH J E. Glucose downregulation of PKG-I protein mediates increased thrombospondin1-dependent TGF- β activity in vascular smooth muscle cells [J]. Am J Physiol Cell Physiol, 2010, 298(5): C1188-C1197.
- [28] LI X C, DING Y, ZI M T, et al. CD19, from bench to bedside[J]. Immunol Lett, 2017, 183: 86-95.
- [29] WENG R Q, LIU S D, GU X D, et al. Clonal diversity of the B cell receptor repertoire in patients with coronary in-stent restenosis and type 2 diabetes [J]. Open Life Sci, 2021, 16(1): 884-898.
- [30] FUJIMOTO M, POE J C, HASEGAWA M, et al. CD19 regulates intrinsic B lymphocyte signal transduction and activation through a novel mechanism of processive amplification[J]. Immunol Res, 2000, 22(2/3): 281-298.
- [31] FUJIMOTO M, FUJIMOTO Y, POE J C, et al. CD19 regulates Src family protein tyrosine kinase activation in B lymphocytes through processive amplification[J]. Immunity, 2000, 13(1): 47-57.
- [32] DEVEZA R C, ELKINS M, SARAGIOTTO B T. PEDro systematic review update: exercise for coronary heart disease[J]. Br J Sports Med, 2017, 51(9): 755-756.
- [33] CHOE N, KWON J S, KIM Y S, et al. The microRNA miR-34c inhibits vascular smooth muscle cell proliferation and neointimal hyperplasia by targeting stem cell factor[J]. Cell Signal, 2015, 27(6): 1056-1065.
- [34] CROTTY S. T follicular helper cell biology: a decade of discovery and diseases[J]. Immunity, 2019, 50(5): 1132-1148.
- [35] PREITE S, HUANG B, CANNONS J L, et al. PI3K orchestrates T follicular helper cell differentiation in a context dependent manner: implications for autoimmunity[J]. Front Immunol, 2018, 9: 3079.